

Effect of Cholesterol on the Properties of Phospholipid Membranes. 1. Structural Features

Pál Jedlovszky*,†

Department of Colloid Chemistry, Eötvös Loránd University, Pázmány Péter sny. 1/a, H-1117 Budapest, Hungary

Mihaly Mezei‡

Department of Physiology and Biophysics, Mount Sinai School of Medicine of the New York University, New York, New York 10029

Received: August 22, 2002; In Final Form: December 12, 2002

All-atom Monte Carlo simulations of four different fully hydrated dimyristoylphosphatidylcholine (DMPC)/cholesterol mixed bilayers have been performed at physiological conditions (i.e., 37 °C and 1 atm). The composition of the different samples has been chosen from both sides of the DMPC/cholesterol miscibility gap; the mole fraction of cholesterol was 0, 0.04, 0.08, and 0.40 in the four systems simulated. The configurations obtained are analyzed in detail, in order to shed some light on the role played by the presence of the cholesterol molecules in the structure of such membranes. It is found that the increase of the cholesterol concentration leads to a decrease of the average area per headgroup, and also to the decrease of the density of the membrane in the crowded region of the headgroups. However, the density in the middle of the membrane is found to be higher when a considerable amount of cholesterol is present in the system. Consistently, the structure in the middle of the membrane is found to be more isotropic, and the two membrane layers are found to approach each other closer in the cholesterol-rich system than in the pure DMPC membrane or in the systems of low cholesterol content. The DMPC molecules, located next to a cholesterol molecule, are found to be more ordered than the ones far from cholesterol. However, this ordering effect of the rigid cholesterol rings on the DMPC tails is found to decrease with increasing cholesterol concentration. As a result, the overall ordering of the DMPC molecules is found to be only rather weakly sensitive to the amount of cholesterol present in the membrane.

Introduction

Cholesterol and its derivatives are crucial components of eukaryotic cell membranes. Their concentration in the membrane of living cells can be as high as 50% in some cases.¹ Besides the phospholipid molecules, cholesterol can thus also be regarded as one of the main constituents of living membranes. Therefore, the investigation of the variation of the properties of phospholipid/cholesterol mixed membranes with changing composition is of great interest, as it is an essential step toward the deep understanding of the structure and biological function of real biological membranes.

Phospholipid molecules are not perfectly miscible with cholesterol; their miscibility gap covers the thermodynamic region typical for the membranes of living cells.^{1–8} For instance, at 37 °C and atmospheric pressure, the immiscibility region of dimyristoylphosphatidylcholine (DMPC) and cholesterol covers the cholesterol mole fraction range of 0.1–0.28.¹ Therefore, in the membranes of living cells, phase separation can occur, resulting in domains of high and low cholesterol concentrations.^{1,4} It is known from experimental studies that cholesterol modifies the properties of pure phospholipid membranes in many ways:⁹ adding cholesterol to a liquid crystal phase phospholipid bilayer reduces the permeability of the membrane,^{10–14} increases its bending elasticity¹⁵ as well as the order of the lipid molecules,^{16,17} and reduces the average area per molecules.^{18,19} The presence of cholesterol reduces or even eliminates the difference between the liquid crystal and gel phase

of the lipid bilayer. Cholesterol also plays a fundamental role as a fluidity regulator of lipid bilayers.^{20,21} In understanding the molecular level origin of these changes, computer simulation can be a very useful tool. In the past decade, several simulations of liquid crystal phase phospholipid membrane systems, including saturated^{22–37} and unsaturated pure lipid bilayers,^{38–43} bilayers containing small dissolved molecules,^{44–47} a transmembrane helix,⁴⁸ or a DNA segment⁴⁹ have been reported. Some of these studies targeted the properties of phosphatidylcholine (PC)/cholesterol mixed bilayers.^{50–57} However, most of these simulations have been performed between 50 and 60 °C,^{50–55,57} usually in compositions falling in the DMPC/cholesterol immiscibility region at body temperature (i.e., 37 °C).^{50,51,53,54,56,57} Only a few simulations have been performed in one of the biologically relevant composition ranges, usually with the cholesterol mole fraction of 0.5.^{52,54,55,57} To our knowledge, only one study has been reported in the cholesterol-poor composition range; in their early work, Edholm and Nyberg have simulated a model membrane containing 3% cholesterol.⁵⁰

In the present paper, we report Monte Carlo simulations of fully hydrated DMPC/cholesterol mixed membranes of different compositions. One of the long-standing goals of our research effort is to find ways to exploit the potential of the Monte Carlo methodology for efficiently sampling the conformational space of biomacromolecules.^{33,58} In a previous study, we have demonstrated that with extension biasing, a novel sampling technique, the sampling efficiency of the Monte Carlo method becomes comparable to that of molecular dynamics on a fully hydrated pure DMPC.³³ The choice of the Monte Carlo methodology has been made with this larger goal in sight.

* E-mail: pali@para.chem.elte.hu.

† E-mail: mezei@inka.mssm.edu.

The composition of the systems simulated has been sampled from both sides of the DMPC/cholesterol miscibility gap. The systems investigated also include a pure DMPC bilayer as a reference system. This work is the first part of a planned series of investigations of the effect of cholesterol molecules on the properties of a DMPC bilayer, and the dependence of these properties on the cholesterol concentration. Thus, here we focus only on the dependence of several structural properties of the membrane on the cholesterol concentration. Besides examining some important features of the overall membrane structure, we are analyzing the effect of cholesterol on the local structure, i.e., how a cholesterol molecule influences the structure of the neighboring lipids. Such changes of the local membrane structure can be rather important in many respects, as they can influence, among others, the solvation and permeability properties of the membrane.

Computational Details

Monte Carlo simulations of fully hydrated DMPC/cholesterol mixed bilayers of different compositions have been performed on the isothermal–isobaric (N, p, T) ensemble at physiological conditions (i.e., at 1 bar and 37 °C). Four systems have been simulated. System I, considered as a reference system, is a bilayer of pure DMPC. Systems II and III contain 4 and 8 mol % cholesterol, respectively. These systems are chosen from the phospholipid-rich side of the DMPC/cholesterol miscibility gap. Finally, system IV is located at the cholesterol-rich side of the immiscibility region containing 40 mol % cholesterol.

The starting configuration of system I, in which each side of the bilayer contains 25–25 DMPC molecules, has been taken from a previous simulation.³⁶ In generating systems II, III, and IV, 1, 2, and 10 randomly chosen DMPC molecules per layer have been replaced by the same number of cholesterol. Each of the four systems has been hydrated by 2033 water molecules. In order to maximize the distance between two periodic images of a given atom in the plane parallel to the bilayer, we have used prism shaped simulation cells having the cross-section of a perfect hexagon. The simulated molecules have been represented by semiflexible all-atom models, in which the bond lengths and bond angles have been kept fixed, whereas torsional flexibility has been included. The geometry and interaction potentials of the DMPC and cholesterol molecules have been taken from the CHARMM22 force field optimized for proteins and phospholipid molecules.⁵⁹ The schematic structures of these molecules, together with the atomic labels used throughout this paper, are shown in Figure 1. The water molecules have been represented by the TIP3P model.⁶⁰ In order to avoid simulating an infinite stack of bilayers, all water–water and water–solute interactions have been truncated to zero at the group-based center–center cutoff distances of 12 and 16 Å, respectively. A similar combination was found to behave close to the infinite cutoff system for a hydrated lipid monolayer.⁶¹ For the solute–solute interactions, a group-based minimum image convention has been used.

The simulations have been performed using the program MMC.⁶² In the simulations, water moving, solute moving, and volume changing steps have been performed. Every water move has been followed by a solute move, and every 625 pairs of such moves by a volume changing step. In a water move, a water molecule has been randomly translated by no more than 0.3 Å and rotated around a randomly chosen space-fixed axis by a random angle below 20°. In choosing the water molecule to be moved, preferential sampling has been applied; i.e., water molecules located closer to the bilayer have been selected with higher probability. In a solute move, either the entire selected

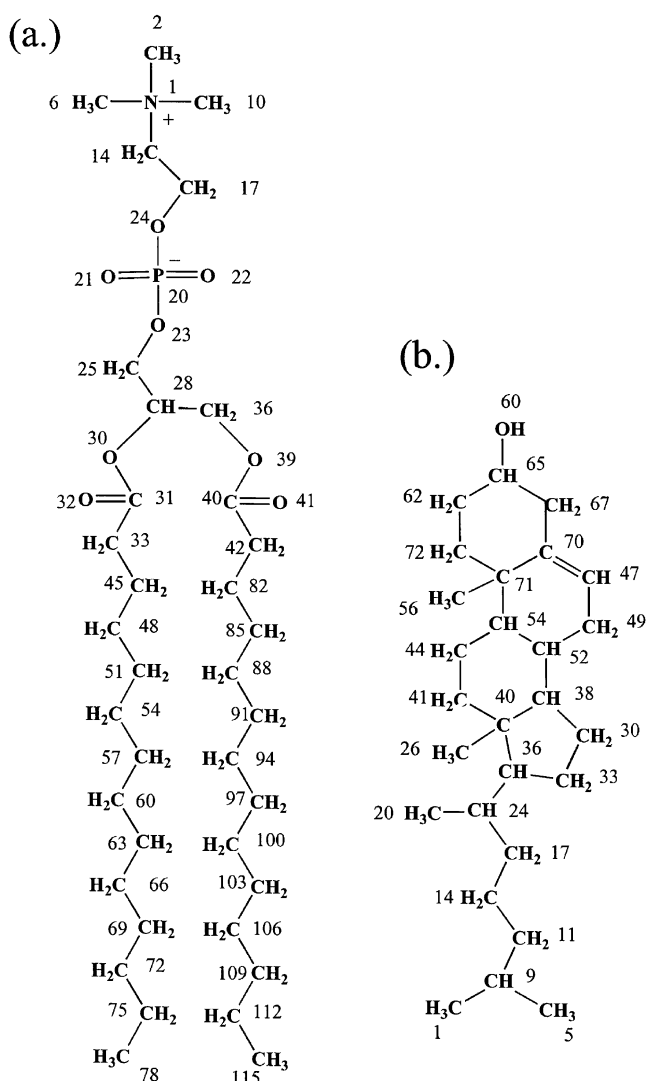


Figure 1. Schematic structure of (a) the DMPC and (b) the cholesterol molecule. The numbering scheme of the heavy atoms used throughout this paper is also indicated.

solute molecule has been translated randomly by no more than 0.05 Å and rotated around a randomly chosen space-fixed axis or one of its torsional angles has been changed. Overall displacements and torsional moves have been chosen with 20% and 80% probabilities, respectively. Solute molecules have been selected for move in a shuffled cyclic order.⁶³ In the torsional moves, the changed torsional angle has been selected in a sequential order going from the end of the chain toward the middle of the molecule. The selection of the torsional angle to be changed has also been subject to a probability filter, allowing less frequent changes of the torsions located near the end of the chains.³³ Overall solute rotations as well as torsional changes have been performed with the novel method of extension biased rotations.³³ In this method, the maximum angle of rotation $\Delta\Phi_{\max}$ depends on the conformation of the rotated molecule or unit. Thus, for each rotation, the R_{\max} distance of the farthest rotated atom from the axis of rotation is determined, and the maximum angle of rotation is calculated as

$$\Delta\Phi_{\max} = \frac{c}{\sqrt{R_{\max}}} \quad (1)$$

where c is the step size parameter, which is kept fixed in the entire simulation. In this way, the smaller the extension of the

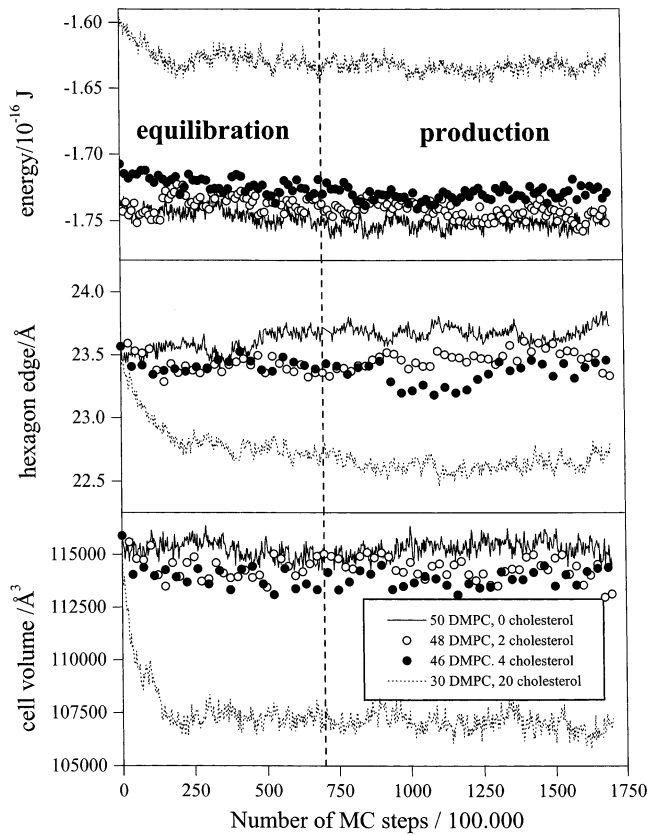


Figure 2. Evolution of the energy, the edge length of the basic hexagon of the simulation cell, and the basic cell volume of the four systems simulated during the simulation runs: solid lines (—), system I; open circles (○), system II; full circles (●), system III; dotted lines (· · ·), system IV. The dashed vertical line separates equilibration and production phases.

rotated unit perpendicular to the rotational axis is, the larger the moves are that can be performed, which improves considerably the sampling from the configurational space of the lipid molecules.³³ In the volume changing steps, either the edge length of the basic hexagon or the height of the prism-shaped simulation box has been changed randomly in such a way that the total volume of the system has not been changed by more than 800 \AA^3 . The two types of volume changes have been attempted in an alternating order. In this way, the surface density of the lipid and cholesterol molecules and the volume density of the entire system have been equilibrated independently from each other, and thus, the pressure in the direction perpendicular to the bilayer is kept equal to the pressure in directions parallel to the bilayer in the entire simulation.⁶⁴ About 50%, 25%, and 35% of the attempted water, overall lipid, and volume changing moves have been accepted, respectively. The rates of the accepted and tried torsional moves have been ranging between about 0.15 and 0.35 for the different torsional angles. The systems have been allowed to equilibrate in 7×10^7 Monte Carlo steps long runs. Then, 1000 sample configurations, separated by 10^5 Monte Carlo steps long runs each, have been saved for further evaluation in each system. The evolution of the energy as well as the edge length of the basic hexagon and the volume of the simulation cell in the simulations is shown in Figure 2 in the four systems. The snapshot of an equilibrium configuration of system IV is shown in Figure 3.

Results and Discussion

Average Structure. The electron density profile as well as the density profile of water and solute heavy atoms in the four

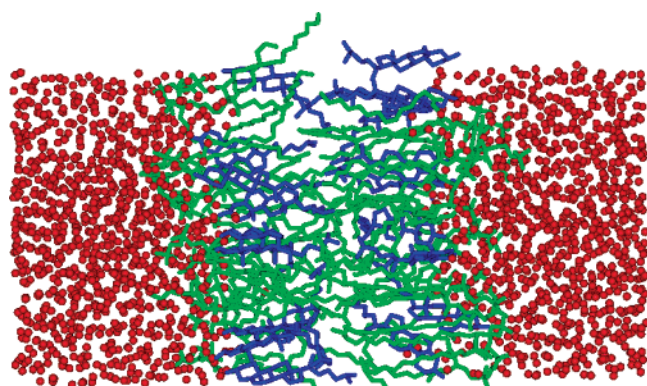


Figure 3. Snapshot showing an instantaneous equilibrium configuration of a fully hydrated DMPC/cholesterol mixed bilayer of 40% cholesterol content (system IV). DMPC, cholesterol, and water molecules are shown in green, blue, and red colors, respectively. For better visualization, H atoms are omitted.

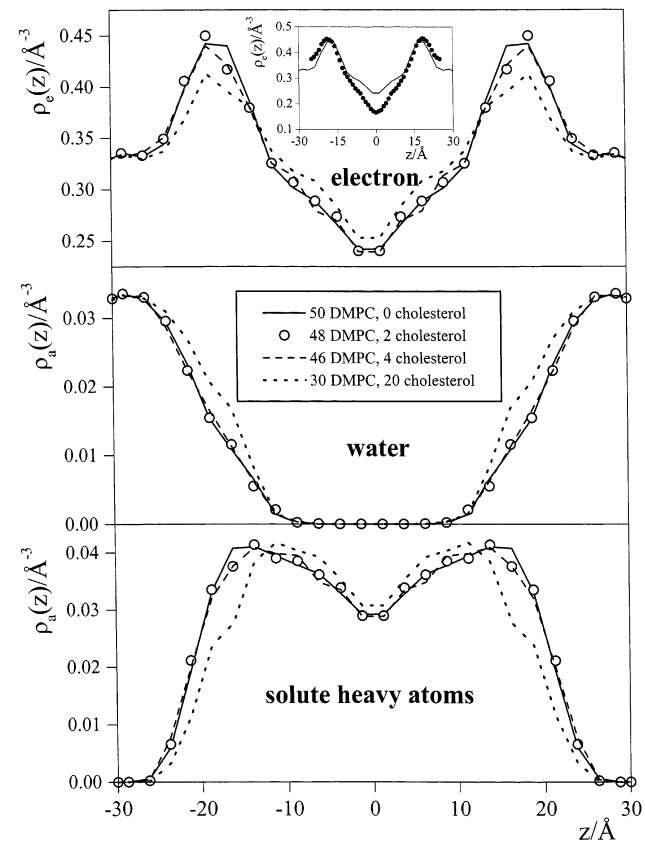


Figure 4. Density profile of various quantities across the simulated membranes. Top: electron density profile. Middle: molecular number density profile of water. Bottom: number density profile of DMPC and cholesterol heavy atoms. Solid lines (—), system I; open circles (○), system II; dashed lines (—), system III; dotted lines (· · ·), system IV. The inset compares the simulated electron density profile of the pure DMPC membrane (—) with results of an X-ray scattering experiment⁶⁵ (●).

systems simulated are shown and compared in Figure 4. For better statistics, the density profiles shown are averaged over the two sides of the bilayers. The obtained electron density profile of the pure DMPC membrane is also compared with experimental data.⁶⁵ The experimental curve is reasonably well reproduced, apart from the depth of the minimum at the middle of the bilayer. However, for the purpose of the following analysis, this discrepancy is probably of minor importance, as in this region the density of the membrane is found to depend

only rather weakly on the composition. Thus, it is reasonable to assume that the dependence of the deviation itself on the composition is also very weak, and hence, it largely cancels out when analyzing the change of the density profile with changing composition. When comparing the profiles obtained in the different systems, it is seen that the presence of a small amount of cholesterol has only an almost negligibly small effect on the average density profiles when compared with the pure DMPC membrane. A similarly small difference has been obtained by Tu et al.⁵³ and by Smolnyrev and Berkowitz⁵⁴ when comparing the simulated electron density profile of mixed dipalmitoylphosphatidylcholine (DPPC)/cholesterol membranes of 12.5% and 11% cholesterol content, respectively, with that of pure DPPC. On the other hand, the average structure of a cholesterol-rich membrane (i.e., system IV) is found to be noticeably different from that of pure DMPC or DMPC-rich mixed membranes. Thus, the presence of a considerable amount of cholesterol in the membrane decreases the density between about 14 and 25 Å along the space-fixed axis perpendicular to the membrane (denoted here as z , $z = 0$ being in the middle of the bilayer) and also slightly increases the density in the middle of the membrane, within about $z = \pm 14$ Å. Thus, in systems I–III, the difference of the highest and lowest electron density values along the z axis has resulted in about 0.20 \AA^{-3} , which is 25% larger than the value of 0.16 \AA^{-3} obtained in system IV. Hence, cholesterol-rich membranes have considerably smaller density variation along the bilayer normal than membranes of low or no cholesterol content.

The comparison of the water and solute heavy atom density profiles shows that in the cholesterol-rich system the lipid and cholesterol molecules can approach the middle of the membrane somewhat closer, realizing a more compact structure in the region of the hydrocarbon chains, than in the other three systems. Consistently, the water density is noticeably higher between 13 and 23 Å in system IV than in the systems of low or no cholesterol content, indicating that more water molecules can penetrate close to the middle of the membrane in the cholesterol-rich system than in the others.

In order to better understand the effect of cholesterol on the average membrane structure, we have also calculated the distribution of various types of atoms along the membrane normal in the cholesterol-rich system. The resulting profiles, averaged over the two sides of the bilayer, are shown in Figure 5. The total electron density profile of this system is also shown here for reference. The maximum of the electron density profile falls between 15 and 25 Å. This is the region where the lipid P and N atoms are located, and where the presence of a large amount of cholesterol decreases the average density. Thus, the presence of a large amount of cholesterol in the membrane decreases the density in the region of the lipid headgroups. However, the contribution of the cholesterol to the total electron density profile is limited to the inner segment of this region as the density distribution of the cholesterol O atoms drops almost to zero at a distance of 20 Å from the middle of the membrane. This effect can be understood considering that the polar group of the cholesterol molecule is considerably smaller than that of DMPC, as cholesterol has only a small OH group as a polar head instead of the large phosphatidylcholine zwitterionic headgroup of DMPC. Hence, a large part of the region of the lipid headgroups is almost inaccessible for cholesterol. It is also seen from the comparison of the various density profiles (Figures 4 and 5) that the space in the lipid headgroup region, created by the lack of a large polar group of cholesterol, is partly filled by water

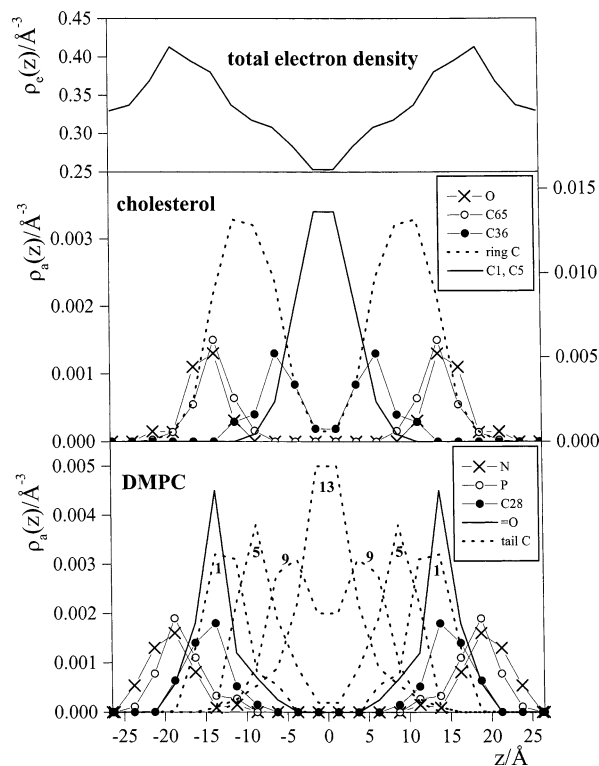


Figure 5. Distribution of atoms of various types along the membrane normal in system IV. Top: total electron density profile of the system, shown for comparisons. Middle: density profile of cholesterol atoms. Crosses (\times), O atom; open circles (\circ), C65 atom; full circles (\bullet), C36 atom; dotted line (\cdots), all C atoms belonging to the ring system; solid line (—), C atoms of the chain terminal CH_3 groups. The scale on the right refers to the density of the ring C atoms. Bottom: density profile of DMPC atoms. Crosses (\times), N atom; open circles (\circ), P atom; full circles (\bullet), C28 atom; solid line (—), carbonyl O atoms; dashed lines (—), tail carbon atoms. The labels 1, 5, 9, and 13 refers to the 1st (i.e., C33 and C42), 5th (C54 and C91), 9th (C66 and C103), and 13th (C78 and C115) tail carbon atoms, respectively.

molecules. Thus, the region between 13 and 23 Å, where the water density is found to be higher in the cholesterol-rich system than in the others, coincides with the layer where the lipid P atoms are located and is just next to the most probable location of the outmost atoms of cholesterol, i.e., the OH group, at $z = 14$ Å.

The increase of the density in the middle of the bilayer due to the presence of a considerable amount of cholesterol can simply be explained, at least partly, by the fact that carbon atoms are more closely packed in a cholesterol ring system than in the hydrocarbon tails of DMPC. Namely, the cholesterol ring system can be regarded as two hydrocarbon “chains” (i.e., C67–C70–C47–C49–C52–C38–C30–C33 and C62–C72–C71–C54–C44–C41–C40–C36, see Figure 1), interconnected by four covalent bonds (i.e., between C70–C71, C52–C54, C38–C40, and C33–C36). Due to this extensive chemical bonding between the two “chains”, a more compact packing of atoms is realized here than in a DMPC molecule, where the two tails are real linear chains, and hence atoms belonging to different chains cannot approach each other closer than the sum of their van der Waals radii. Furthermore, being already restrained by chemical bonds, the two “chains” do not have to pay an entropic penalty for being so close all the time. This more compact way of packing the atoms in a cholesterol molecule as well as the effect of the lack of the large cholesterol headgroup leads also to a lateral contraction of the system. This is indicated by the decrease of the equilibrium edge length of the basic hexagon

of the simulation cell (see Figure 2), as well as by the decrease of the average headgroup area per molecule with increasing fraction of cholesterol in the membrane. The latter values resulted in 58.2, 57.0, 56.7, and 53.2 Å² in systems I, II, III, and IV, respectively.

The atomic distributions shown in Figure 5 provide also some information on the average structure of the hydrocarbon region of the membrane. Thus, it is seen that the carbonyl O atoms of the DMPC molecules are located at about $|z| = 15$ Å with the highest probability. The most probable locations of the cholesterol C36 and C65 atoms (i.e., the two endpoints of the ring system) are found at about 6 and 14 Å from the middle of the membrane, respectively, and thus, a majority of the cholesterol ring C atoms are in this z range. The chain terminal CH₃ groups of both the DMPC and the cholesterol molecules are located within about 5 Å from the middle of the membrane. No considerable difference is seen between the distributions of these methyl groups of DMPC and of cholesterol. All these findings are consistent with our stated conclusions and indicate that the apolar parts of the two molecules are roughly equally long, and both molecules can approach the middle of the membrane with about the same probability. This feature is in contrast with the properties of mixed PC/cholesterol membranes of larger lipid molecules, such as DPPC. In such membranes, the lipid tails are considerably longer than the cholesterol molecules, and hence, cholesterol is not able to access the middle of the bilayer. This difference between DMPC and DPPC can be responsible for the marked difference between the electron density profile of our cholesterol-rich system and that of the 1:1 DPPC/cholesterol mixed bilayer, as obtained by Smolnyrev and Berkowitz using a different force field.⁵⁴ Namely, in the latter system, the density drops sharply within the distance of about ± 4 Å from the middle of the bilayer (i.e., in the region inaccessible by cholesterol) and becomes even lower than the density of the pure DPPC membrane here (see Figure 8 of ref 54).

It is also seen from Figure 5 that the distribution of the cholesterol O atoms along the membrane normal is very similar to that of the C_β atoms of the DMPC glycerol backbone (denoted as C28 atom according to the atom numbering scheme shown in Figure 1). This finding is also in agreement with results of previous simulations of both DMPC/cholesterol⁵⁶ and DPPC/cholesterol^{53,54} mixed membranes of various compositions. The similarity between the spatial distribution of the cholesterol O and DMPC C28 atoms is even more evident from Figure 6, which shows the distributions of the thickness of the cholesterol-rich membrane d , measured between the average position of selected cholesterol and DMPC atoms in the two sides of the bilayer. The distributions of both the cholesterol O–O and the DMPC C28–C28 thicknesses are centered around 30 Å and almost completely overlap each other. This similarity between the distribution of cholesterol O and DMPC C28 atoms along the membrane normal can be explained by the rather complex hydrogen bonding structure between cholesterol and the adjacent lipid molecules. Namely, the cholesterol OH group can interact both with the lipid carbonyl and phosphate groups either through a direct hydrogen bond or through a water bridge (see Figure 10 of ref 56 for the possible types of lipid–cholesterol hydrogen bonds), and hence, a cholesterol molecule can be strongly connected to its lipid neighbors by several hydrogen bonds.⁵⁶ This complex hydrogen bonding structure anchors the cholesterol headgroups at about the same z value where the lipid C28 atoms are located (i.e., between the lipid carbonyl and phosphate oxygens).

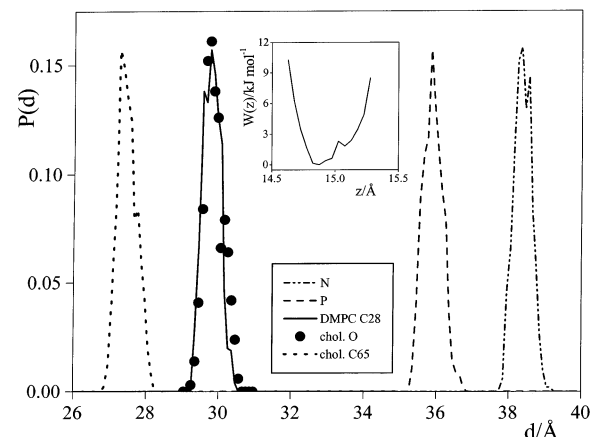


Figure 6. Distribution of the membrane thickness d , measured as the distance between the average positions of specific atoms in the two sides of the bilayer, in system IV. Solid line (—), DMPC C28–C28 thickness; dashed line (—), P–P thickness; dash-dotted line (---), N–N thickness; dotted line (···), cholesterol C65–C65 thickness; full circles (●), cholesterol O–O thickness. The inset shows the potential of mean force W acting on a cholesterol molecule the O atom of which is located at a distance z from the middle of the bilayer along the membrane normal.

The inset of Figure 6 shows the potential of mean force W acting on a cholesterol molecule as a function of the distance of its O atom from the middle of the membrane along the z axis in system IV. The $W(z)$ function has been derived from the $P(d_{O-O})$ distribution of the cholesterol O–O thickness of this membrane as

$$W(z) = W\left(\frac{d_{O-O}}{2}\right) = -RT \ln[P(d_{O-O})] + C \quad (2)$$

where R is the gas constant and C is an arbitrary additive constant, the value of which has been chosen in such a way that the minimum of the $W(z)$ function corresponds to zero energy. The $W(z)$ function can only be determined in this way in the z range where the corresponding $P(d_{O-O})$ distribution is not zero. The determined $W(z)$ potential of mean force function can be extended to a considerably broader z range by performing a Monte Carlo simulation in which adaptive umbrella sampling^{66,67} is used for sampling the z coordinate of a given cholesterol molecule. Work in this direction is currently in progress.

This anchoring of the cholesterol headgroups at a certain z range can help to explain the observed thinning of the hydrocarbon phase of the membrane in the presence of a large amount of cholesterol (see Figure 4). The cholesterol molecule has only one tail, and therefore, the replacement of a DMPC molecule by cholesterol, although leading to higher density in the region of the ring system, creates some empty space in the middle of the membrane. On the other hand, the anchoring of their OH groups by hydrogen bonds to the nearby lipid molecules prevents the cholesterol from moving toward the middle of the bilayer and filling this space. Instead, this space is filled by getting the two entire membrane layers closer to each other, which results in the observed thinning effect.

Effect of a Nearby Cholesterol on the Local Lipid Structure. *Arrangement of the Molecules Along the Membrane Normal.* In order to investigate the effect of cholesterol on the organization of the DMPC molecules along the membrane normal, we have compared the C28–C28 thickness of the membranes containing 0%, 8%, and 40% cholesterol (see Figure 7). The obtained results are rather surprising, as the average

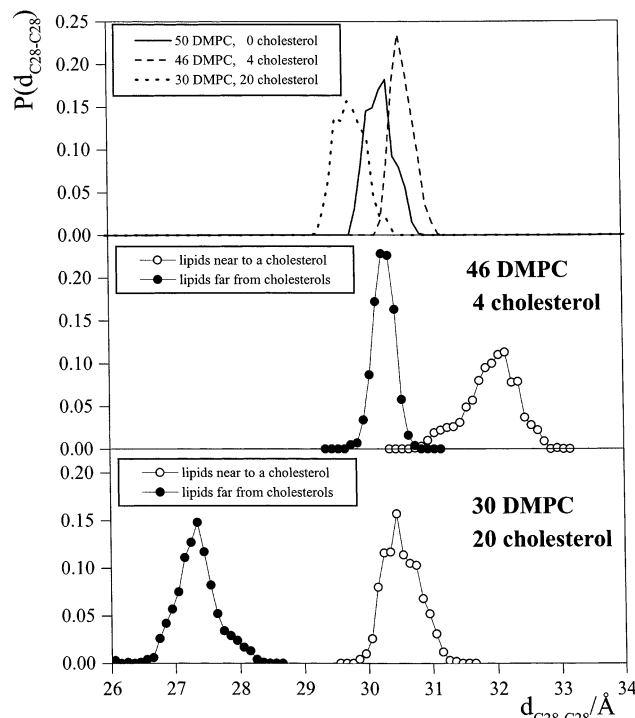


Figure 7. Distribution of the DMPC C28–C28 thickness $d_{C28-C28}$ (defined as the distance of the average position of the C28 atoms on the two sides of the bilayer) of the DMPC/cholesterol mixed membranes. Top: thickness of system I (—), system III (—), and system IV (· · ·). Middle: comparison of the C28–C28 thickness of DMPC molecules located near (i.e., closer than the lateral center of mass–center of mass distance of 8.0 Å) to a cholesterol (○) and far from cholesterol (●) in system III. Bottom: comparison of the C28–C28 thickness of DMPC molecules located near to a cholesterol (○) and far from cholesterol (●) in system IV.

thickness resulted in 30.2 ± 0.2 , 30.6 ± 0.2 , and 29.8 ± 0.2 Å in systems I, III, and IV, respectively. Hence, in the presence of a small amount of cholesterol, the $d_{C28-C28}$ thickness of the membrane becomes larger than that in pure DMPC (i.e., the C28 atoms are farther from the middle of the bilayer), whereas in the cholesterol-rich membrane an opposite effect is observed: this membrane is thinner than the pure DMPC bilayer according to the distance of the average positions of the C28 atoms in the two layers. This latter finding is in accordance with the observed behavior of the electron density and solute heavy atom profiles (see Figure 4) and is also in agreement with the findings of Tu et al. for a DPPC/cholesterol mixed bilayer,⁵³ described by a force field different from the one used here. A similar effect has been seen for the P–P and the N–N thickness of the membranes studied, indicating that the observed behavior is not specific only for the glycerol backbone of the DMPC molecules.

In order to understand the observed change of the membrane thickness with increasing concentration of cholesterol, we have divided the DMPC molecules into two separate groups according to whether they have a nearest lateral cholesterol neighbor or not. Therefore, the centers of mass of the DMPC and cholesterol molecules, located in the same layer, have been projected to the xy plane (i.e., the plane of the membrane). A DMPC molecule is regarded as a “DMPC near to a cholesterol”, if the projection of its center of mass is closer than 8 Å to that of the nearest cholesterol molecule, and is called as a “DMPC far from cholesterol” otherwise. The limiting distance value of 8 Å has been chosen because the projections of the cholesterol centers of mass are, on average, two-coordinated by the projections of

the DMPC centers of mass within this distance. Hence, the present definition of the “DMPC close to a cholesterol” mostly selects the DMPC molecules which are linked to a cholesterol by hydrogen bonds. These definitions of DMPC molecules located close to a cholesterol and far from cholesterol are used throughout this paper. This definition yielded an average number of 4, 9, and 23 lipids near to a cholesterol, and 44, 37, and 7 lipids far from cholesterol in systems II, III, and IV, respectively. It should be noted that the cholesterol centers of mass are located, on average, about 2.5 Å closer to the middle of the membrane than the centers of mass of the DMPC molecules. In order to exclude the possibility that this slight difference between the average position of the DMPC and cholesterol centers of mass along the z axis results in an improper determination of the DMPC molecules which do and which do not have a near cholesterol neighbor, we have repeated the procedure by projecting the lipid C28 and cholesterol O atoms instead of the centers of mass to the xy plane. The list of the lateral DMPC–cholesterol contact pairs obtained this way is found to be essentially identical to the one obtained when the molecular centers of mass have been projected.

The distributions of the C28–C28 distance of DMPCs located close to a cholesterol and far from cholesterol are shown separately for systems III and IV in Figure 7. As is seen, in the case of 8% cholesterol content, the distribution of the $d_{C28-C28}$ thickness of the lipids which are far from cholesterol is very similar to the distribution observed in pure DMPC. Therefore, the increase of the C28–C28 thickness due to the presence of a small amount of cholesterol is exclusively due to the lipids which are located next to a cholesterol molecule. As has been discussed already, the presence of a cholesterol molecule in the membrane creates some space in the headgroup region because of the lack of its large polar head. In the presence of a considerable amount of cholesterol, this effect leads to a noticeable decrease of the density, and also to an increased penetration of water in this region (see Figure 4). (It should be noted that although no such changes of the average structure have been seen for the mixed membranes of low cholesterol content, this is just because these effects are too small to be observed in our simulation when only a few cholesterol are present in the system.) It has also been discussed already that cholesterol are linked to the neighboring DMPC molecules by hydrogen bonds, and hence, the lone cholesterol molecule itself cannot get closer to the aqueous phase to fill this space. However, this space created by the lack of the large cholesterol head in the headgroup region can, at least partly, be filled by getting the entire hydrogen bonded complex of the cholesterol and its neighboring lipids closer to the aqueous phase. This effect results in the observed large C28–C28 thickness of the DMPC molecules which are close to a cholesterol in system III. This correlation between the arrangement of the cholesterol and neighboring DMPC molecules along the bilayer normal is also confirmed by the fact that the average C28–C28 thickness of DMPCs located next to a cholesterol in system III is 31.9 ± 0.4 Å, which agrees excellently with the cholesterol O–O thickness of 31.8 ± 0.2 Å of this system.

When comparing the distribution of the C28–C28 distance of lipids near to and far from cholesterol in the cholesterol-rich mixed membrane (see the bottom of Figure 7), a difference similar to that in system III is observed. The distribution corresponding to DMPCs located next to a cholesterol again appears at considerably higher values than that of the DMPCs which are far from cholesterol. The mean value and standard deviation of these distributions resulted in 30.5 ± 0.3 and 27.4 Å, respectively.

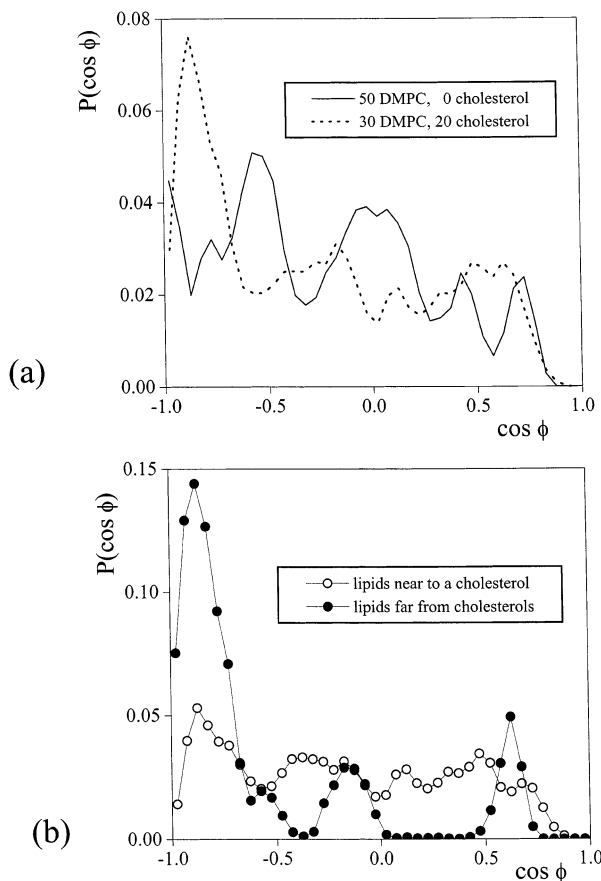


Figure 8. Cosine distribution of the angle ϕ formed by the vector pointing from the P to the N atom of a DMPC molecule (PN vector), and the bilayer normal vector z , pointing toward the middle of the membrane. (a) Comparison of system I (—) and system IV (···). (b) Comparison of the PN vector orientation of lipids located near to a cholesterol molecule (○) and far from cholesterol (●) in system IV.

± 0.4 Å, respectively. This indicates that, similarly to system III, the DMPC molecules having a near cholesterol neighbor are located, on average, considerably farther from the middle of the membrane than DMPCs which are far from cholesterol also in system IV. However, both distributions are shifted toward smaller distances relative to the corresponding distributions in system III, due to the thinning and condensation of the hydrocarbon phase of the membrane in the cholesterol-rich mixture, as discussed in the previous subsection. This thinning effect is strong enough to move the $P(d_{C28-C28})$ distribution of all lipid molecules to smaller values than what is found in the pure DMPC bilayer. Hence, the presence of a large amount of cholesterol in the membrane results in an opposite change of the $C28-C28$ thickness relative to the pure DMPC system than the presence of only a small amount of cholesterol.

Orientation of Molecular Vectors Relative to the Membrane Normal. *A. The PN Vector.* The correlated arrangement of the cholesterol molecules and their DMPC neighbors along the bilayer normal affects also the headgroup structure of the DMPC molecules. The cosine distribution of the angle ϕ formed by the vector pointing from the P to the N atom of a DMPC molecule (PN vector) and the bilayer normal vector pointing toward the middle of the membrane (z vector) is compared in Figure 8a as obtained in the pure DMPC and in the cholesterol-rich mixed membrane. As is seen, the PN vectors have a considerably stronger preference for pointing almost straight to the aqueous phase, and also a stronger preference for pointing back toward the middle of the membrane in system IV than in

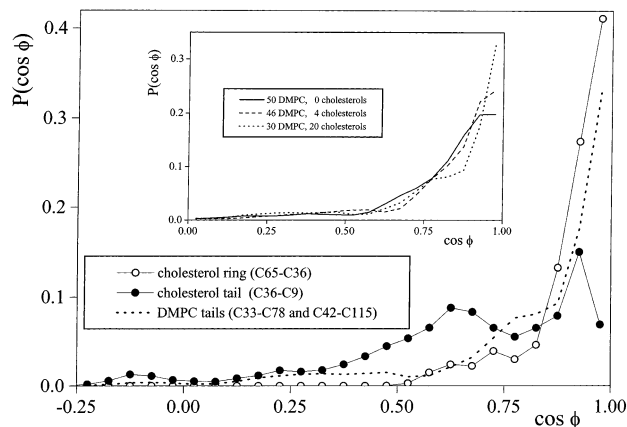


Figure 9. Cosine distribution of the tilt angle ϕ of the direction of the cholesterol ring system, described by the molecular vector pointing from C65 to C36 (○), the cholesterol tail, described by the vector pointing from C36 to C9 (●), and the DMPC tails, described by the vectors pointing from C33 to C78 and from C42 to C115 (···) relative to the bilayer normal vector z , pointing toward the middle of the membrane in system IV. The inset compares the distribution of $\cos \phi$ for the DMPC tails in system I (—), system III (—), and system IV (···).

the cholesterol-free system. On the other hand, lateral directions of the PN vector are preferred stronger in system I than in system IV. In order to understand this effect, we have separated the contribution of the lipids which are close to a cholesterol from those which are far from cholesterol to this distribution in system IV. The separate contributions of the two kinds of DMPC molecules are compared in Figure 8b. The distribution given by the lipids located next to a cholesterol is rather flat in almost the entire $\cos \phi$ range. This distribution is, in general, rather similar to the one observed in the pure DMPC membrane. On the other hand, the distribution given by the lipids which are far from cholesterol has a huge peak near to the $\cos \phi$ value of -1 and another sharp peak above 0.5 , whereas it is always below the other distribution in the $\cos \phi$ range between these two peaks, being zero in a large part of this range of intermediate $\cos \phi$ values. The obtained results are in a clear agreement with the correlated arrangement of the cholesterol and neighboring DMPC molecules, discussed in the previous subsection. Thus, the DMPCs located far from cholesterol are, on average, closer to the middle of the membrane than DMPCs which are next to a cholesterol. In a cholesterol-rich membrane, where only a small fraction of the molecules are DMPCs far from cholesterol, these molecules are surrounded by hydrogen-bonded complexes of cholesterol and their DMPC neighbors. These surrounding hydrogen-bonded molecular complexes are located closer to the aqueous phase than the central DMPC molecule which is far from cholesterol. Therefore, the headgroup of these molecules is largely prevented from being extended in lateral directions by the neighboring hydrogen-bonded complexes, and the likely shape of the free volume pocket available for these headgroups is a long channel perpendicular to the interface. Consistently, the PN vectors of these molecules point rather straight to the aqueous phase (about 70% of the DMPCs located far from cholesterol have an angle larger than 130° between its PN vector and z), and the few PN vectors which turn back to the hydrocarbon phase point also as straight to the middle of the membrane as possible.

B. Hydrocarbon Tails. Figure 9 shows the cosine distribution of the tilt angle of the cholesterol ring system, the cholesterol tail, and the DMPC tails relative to the bilayer normal. These tilt angles are defined as the angle of the vector z with the vector

pointing from the cholesterol C65 to C36, from the cholesterol C36 to C9, and from the DMPC C33 to C78 or C42 to C115 atoms, respectively. The cholesterol rings as well as the DMPC tails are found to strongly prefer parallel alignment with the membrane normal. Obviously, this preference is stronger for the rigid cholesterol rings, which cannot deviate considerably from this preferred orientation. Thus, about 80% of the cholesterol rings have a tilt angle smaller than 30°, and for 40% of them, this angle is even smaller than 15°. Moreover, this tilt angle of the cholesterol rings has never found to be larger than 60°. On the other hand, about 10% of the lipid tails has a tilt angle larger than 60°, and only 60% and 30% of them has a tilt angle smaller than 30° and 15°, respectively. It should also be noted that, contrary to the statement of Chiu et al.,⁵⁷ the most probable value of the tilt angle (which is not the same as its average value) is 0° for both the cholesterol rings and lipid tails. One should be aware that, similar to the angle formed by any two spatial vectors, it is more meaningful to calculate the distribution of these tilt angles as cosine rather than angular distributions, because only the cosine distribution of the angle formed by two uniformly distributed spatial vectors is uniform.

The cosine distribution of the cholesterol tails is considerably less sharp than the other two distributions, as it fluctuates around a constant value between about 0.6 and 1 (i.e., between about 0° and 50°). This tilt angle is smaller than 15° and 30° for only about 7% and 30% of the molecules, respectively. On the other hand, 25% of the cholesterol tails have a tilt angle larger than 60°, and for 4% of them, this angle is even larger than 90°; i.e., the tail turns back pointing toward the aqueous phase. This difference between the tilt angle distribution of the DMPC tails and cholesterol rings and that of the cholesterol tails clearly shows that the structure of the hydrocarbon phase is different in the middle of the membrane from that in the region of the cholesterol rings. The middle of the membrane is considerably more isotropic than the outer region of the hydrocarbon phase. It is reasonable to assume that this isotropy is stronger in membranes of higher cholesterol content, as the lack of the second cholesterol tail in this region facilitates the extension of the tails in lateral directions. This point is analyzed further in the following subsection. On the other hand, in the outer part of the hydrocarbon phase, the membrane is more ordered, and this order is further increased by the presence of the rigid cholesterol rings. This is illustrated in the inset of Figure 9, which compares the tilt angle cosine distribution of the DMPC tails in systems I, III, and IV. As is clearly seen, the distribution becomes sharper with increasing cholesterol concentration. This difference between the structure of the outer and inner part of the hydrocarbon phase is in a clear accordance with the findings of the detailed free volume analysis of a pure DPPC bilayer of Marrink et al.⁶⁸ and can be responsible for the permeability properties of these membranes.^{23,68,69}

Local Structure of the DMPC Tails. The local order of the DMPC tails at different depths in the membrane can be characterized by the deuterium order parameter profile of the chains. This profile can also be accessed experimentally, by NMR measurement of a deuterated sample. The deuterium order parameter S_{CD} at a given C atom of a DMPC tail can be calculated in the simulation as

$$S_{CD} = \left\langle \frac{3}{2} \cos^2 \alpha - \frac{1}{2} \right\rangle \quad (3)$$

where α is the angle formed by the C–D bond and the bilayer normal, and the brackets $\langle \dots \rangle$ denote ensemble averaging. The obtained S_{CD} profiles of the DMPC molecules, averaged over

the two tails, are shown in Figure 10a in the four systems simulated. The profile obtained in pure DMPC is also compared here with experimental data.⁷⁰ The order parameter profiles given by only those DMPC molecules which are located near to a cholesterol as well as by those which are far from cholesterol are also compared separately in the different systems in Figure 10. Obviously, in the pure DMPC membrane all of the molecules are regarded as being far from cholesterol. It should be noted that in Figure 10 the chain carbon atoms are numbered from the middle of the DMPC molecule toward the end of the chains; i.e., the C33 and C42 atoms are regarded as the first and the chain terminal C78 and C115 atoms as the last (13th) tail C atoms.

The experimental S_{CD} profile of pure DMPC is rather well reproduced in the simulation along the entire chain apart from its first CH_2 group. When the profiles obtained in different systems are compared, rather little difference is seen. The order parameters increase slightly with increasing cholesterol concentration at the first five CH_2 groups along the tails. As seen from Figure 5, these methylene groups are located at about the same depth along the z axis as the cholesterol rings. Upon approaching the middle of the membrane, the order parameters are found to decrease sharply in each of the four systems, indicating again that the hydrocarbon phase becomes less ordered toward the middle of the membrane. When the S_{CD} profiles of the DMPC molecules located near to a cholesterol in the different mixed systems are compared, a more marked difference is found. The order of these molecules, in particular between the 5th and 11th CH_2 groups, is clearly higher in systems of lower cholesterol content. On the other hand, the cholesterol content of the membrane has no influence on the order of the tail of the DMPC molecules which are located far from cholesterol, at least in systems of low cholesterol content. In system IV, these DMPC molecules show slightly higher order at the first three CH_2 groups and somewhat lower order at the middle of the chains. However, in interpreting these differences, one should be aware that in the cholesterol-rich system only a few DMPC molecules are far from cholesterol, and hence, the statistical uncertainty of their S_{CD} profile is rather large.

The S_{CD} profile of the DMPC molecules which are located near to a cholesterol and of those which are far from cholesterol are compared in Figure 10b in all the three mixed systems. This comparison clearly reveals that the presence of a nearby cholesterol molecule increases the order of the lipid tails. However, this effect becomes weaker at higher cholesterol concentrations, as the difference between the two profiles becomes smaller from system II to system IV. It should be noted that similar behavior of the deuterium order parameter has recently been found by Domínguez in a system of surfactant mixtures adsorbed at the water/CCl₄ interface, where the presence of one of the surfactants increases the order of the neighboring molecules of the other type, but this ordering effect becomes weaker with increasing concentration of the first type of surfactants.⁷¹ The reason for the observed behavior is probably that the rigid cholesterol ring system induces some extra order on the nearby DMPC tails; however, the alignment of the cholesterol rings is uncorrelated, and hence, the increase of the cholesterol concentration in the membrane does not lead to an increased order of the lipid tails.

Besides the order parameters, the structure of the DMPC hydrocarbon tails can also be characterized by the orientation of the individual C–C bonds along the chains. Figure 11a shows the profile of the average cosine value of the angle γ formed by a C–C bond and the bilayer normal. The obtained profiles

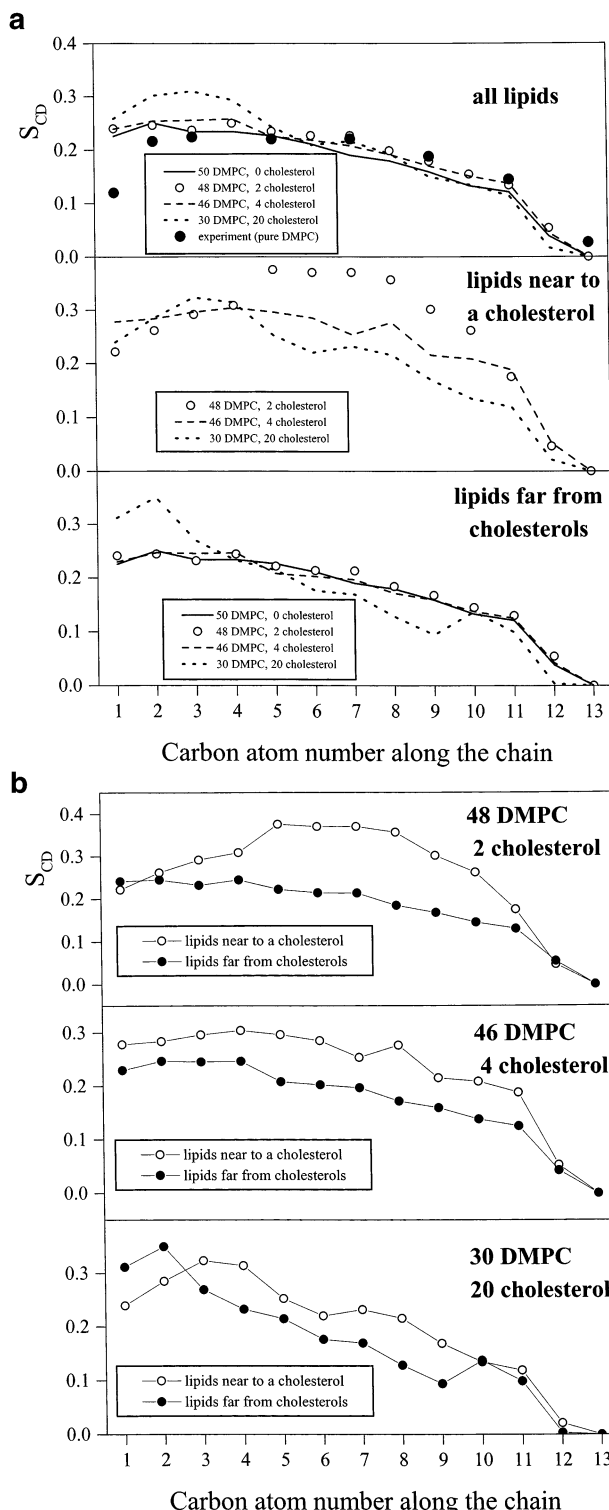


Figure 10. Deuterium order parameter profiles along the DMPC tails in the four systems simulated. (a) Comparison of the profiles in different systems. Top: profiles obtained for all DMPC molecules. Middle: profiles obtained for DMPC molecules located near to a cholesterol. Bottom: profiles obtained for DMPC molecules located far from cholesterol. Solid lines (—), system I; open circles (○), system II; dashed lines (—), system III; dotted lines (· · ·), system IV. The full circles (●) in the top panel show experimental data obtained on a pure DMPC membrane.⁷⁰ (b) Comparison of the profiles obtained for DMPC molecules located near to a cholesterol (○) and for DMPCs located far from cholesterol (●) in the three mixed systems. Top, system II; middle, system III; bottom, system IV. The C—C bonds of the DMPC tails are numbered from the middle of the molecule (i.e., from C33 and C42) toward the end of the tails.

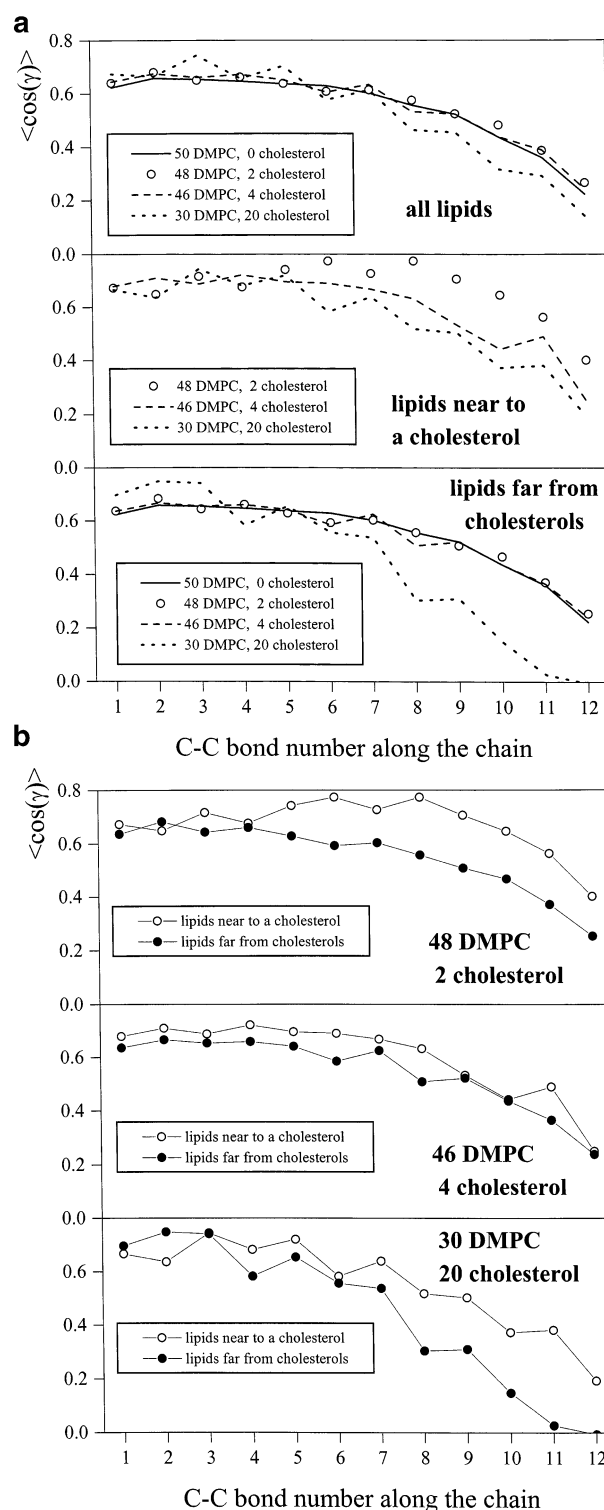


Figure 11. Profiles of the average cosine of the angle γ , formed by a C—C bond of a DMPC tail and the membrane normal, along the DMPC tails in the four systems simulated. (a) Comparison of the profiles in different systems. Top: profiles obtained for all DMPC molecules. Middle: profiles obtained for DMPC molecules located near to a cholesterol. Bottom: profiles obtained for DMPC molecules located far from cholesterol. Solid lines (—), system II; open circles (○), system III; dashed lines (—), system IV; dotted lines (· · ·), system I. (b) Comparison of the profiles obtained for DMPC molecules located near to a cholesterol (○) and for DMPCs located far from cholesterol (●) in the three mixed systems. Top, system II; middle, system III; bottom, system IV. The C—C bonds of the DMPC tails are numbered from the middle of the molecule (i.e., from the C33—C45 and C42—C82 bonds) toward the end of the tails.

are again compared for all DMPC molecules as well as for DMPCs located near to a cholesterol and for those which are far from cholesterol. The $\langle \cos \gamma \rangle$ profiles of the lipids which are close to a cholesterol and of those which are far from cholesterol are compared in Figure 11b in each of the three mixed systems. The C–C bonds of the tails are again numbered from the middle of the DMPC molecule toward the end of the tails.

The $\langle \cos \gamma \rangle$ profiles of all DMPC molecules show little differences in the different systems. The only noticeable effect of the membrane composition on this profile is that in the case of the cholesterol-rich membrane the $\langle \cos \gamma \rangle$ value is somewhat smaller for the last five bonds, indicating weaker preference of these bonds for a parallel alignment with the membrane normal than in the other three systems. It is also seen that the $\langle \cos \gamma \rangle$ values are decreasing toward the end of the tails in all the four systems, and this decrease is stronger in the cholesterol-rich system than in the others. This finding is consistent with our previous results, indicating again that the structure of the hydrocarbon phase becomes more isotropic toward the middle of the membrane, and this effect is stronger in membranes of high cholesterol content.

Similar behavior is seen when the $\langle \cos \gamma \rangle$ profiles of only those DMPC molecules are compared in the different systems, which are far from cholesterol. The difference between the $\langle \cos \gamma \rangle$ values of the cholesterol-rich and the other three systems at the end of the tails is, however, considerably larger here than when all the DMPC molecules are considered. It is quite remarkable that the preference for being parallel with the membrane normal vanishes completely for the last two C–C bonds of the tails of the DMPC molecules located far from cholesterol in system IV. It is also seen from Figure 11b that the C–C bonds of the lipids which are close to a cholesterol molecule are pointing, on average, consistently more straight toward the middle of the membrane than the corresponding C–C bonds of the lipids which are far from cholesterol. Hence, cholesterol has a dual effect on the orientational order of the C–C bonds of the DMPC tails. On one hand, the presence of a nearby cholesterol increases the orientational order of the C–C bonds along the entire DMPC tails, whereas, on the other hand, the increase of the cholesterol content of the membrane decreases the average order of the C–C bond orientation in the middle region of the bilayer.

Summary and Conclusions

In analyzing the difference between the structure of DMPC/cholesterol mixed membranes of various compositions, we have found that these differences originate in the different molecular structure of DMPC and cholesterol, and also in the specific interaction between neighboring DMPC and cholesterol molecules. As it has been investigated in detail by Pasenkiewicz-Gierula et al.,⁵⁶ cholesterol molecules can interact with their DMPC neighbors through various different hydrogen bonding schemes and form strong hydrogen bonding complexes with these neighbors. Cholesterol is anchored by these hydrogen bonds to a certain depth along the membrane normal axis z , as their position along the membrane normal is strongly correlated with that of their nearest DMPC neighbors.

The main differences between the molecular structure of cholesterol and DMPC, relevant in determining the structure of the membrane, are (i) the lack of the large polar headgroup of cholesterol, (ii) the fact that the atoms are packed in a more compact way in the cholesterol ring system than in the hydrocarbon tails of DMPC, as the two “tails” are interconnected

by four C–C bonds in cholesterol, and (iii) the lack of the second cholesterol tail next to the ring system, in the middle part of the bilayer. These differences, together with the ability of cholesterol to form strongly hydrogen bonded complexes with their DMPC neighbors, lead to the observed lateral condensation of the membrane (i.e., the decrease of the average area per headgroup) with increasing cholesterol concentration. The lack of the large polar head and the second tail of cholesterol leads to the increase of the free volume in the region of the headgroups and in the middle part of the membrane, respectively, when a DMPC molecule is replaced by cholesterol. This extra free volume is decreased by the lateral condensation in both regions. In addition, in the dense headgroup region it leads to an increased water penetration, and also to the fact that the entire hydrogen bonded complexes formed by cholesterol and their nearest DMPC neighbors can get closer to the aqueous phase than those DMPCs which are far from cholesterol. Moreover, the overall density of this region is also decreased in the presence of a considerable amount of cholesterol.

Contrary to the crowded region of the headgroups, the density in the middle region of the membrane is rather low. The DMPC tails are about as long as the cholesterol molecules, and hence, the chain terminal CH_3 groups of the two molecules are distributed in the same way along the z axis. Therefore, the lack of the second cholesterol tail in this region allows the two layers to get closer to each other, as it facilitates the extension of the hydrocarbon chains also in lateral directions. This condensation effect along the membrane normal (i.e., thinning of the bilayer), together with the lateral condensation, leads to an overall increase of the density in the middle of the membrane in the presence of a considerable amount of cholesterol.

When analyzing the effect of cholesterol molecules on the local structure of their nearest DMPC neighbors, we have found that the rigid cholesterol ring system induces some extra order on the hydrocarbon tail of the nearest DMPC molecules. However, this extra order induced by cholesterol is not correlated between the environment of different cholesterol molecules, and hence, the difference between the order of DMPC molecules located next to a cholesterol and of those which are far from cholesterol decreases consistently with increasing cholesterol concentration.

Acknowledgment. P.J. is a Magyary Zoltán fellow of the Foundation for Hungarian Research and Higher Education, Ministry of Education, Hungary, which is gratefully acknowledged. P.J. acknowledges support of the Hungarian OTKA Foundation under Project F038187 and of INTAS under Project 2001-0067. The authors also acknowledge access to the computer facilities at the Institute of Computational Biomedicine (ICB) of the Mount Sinai Medical Center.

References and Notes

- (1) Sackmann, E. In *Structure and Dynamics of Membranes*; Lipowsky, R., Sackmann, E., Eds.; Elsevier: Amsterdam, 1995; pp 1–64.
- (2) Vist, M. R.; Davis, J. H. *Biochemistry* **1990**, *29*, 451.
- (3) McMullen, T. P. W.; McElhaney, R. N. *Biochim. Biophys. Acta* **1995**, *1234*, 90.
- (4) Slotte, J. P. *Biochim. Biophys. Acta* **1995**, *1238*, 118.
- (5) Radhakrishnan, A.; McConnell, H. M. *J. Am. Chem. Soc.* **1999**, *121*, 486.
- (6) Radhakrishnan, A.; McConnell, H. M. *Biophys. J.* **1999**, *77*, 1507.
- (7) Keller, S. L.; McConnell, H. M. *Phys. Rev. Lett.* **1999**, *82*, 1602.
- (8) Richter, F.; Finegold, L.; Rapp, G. *Phys. Rev. E* **1999**, *59*, 3483.
- (9) McMullen, T. P. W.; McElhaney, R. N. *Curr. Opin. Colloid Interface Sci.* **1996**, *1*, 83.
- (10) Carruthers, A.; Melchior, D. L. *Biochemistry* **1983**, *22*, 5797.
- (11) Bittman, R.; Clejan, S.; Lund-Katz, S.; Phillips, M. C. *Biochim. Biophys. Acta* **1984**, *772*, 117.

(12) Subczynski, W. K.; Hyde, J. S.; Kusumi, A. *Proc. Natl. Acad. Sci. U.S.A.* **1989**, *86*, 4474.

(13) Subczynski, W. K.; Wisniewska, A.; Yin, J.-J.; Hyde, J. S.; Kusumi, A. *Biochemistry* **1994**, *33*, 7670.

(14) Xiang, T.-X.; Anderson, B. D. *Biophys. J.* **1997**, *72*, 223.

(15) Mélard, P.; Gerbeaud, C.; Pott, T.; Fernandez-Puente, L.; Bivas, I.; Mitov, M. D.; Dufourcq, J.; Bothorel, P. *Biophys. J.* **1997**, *72*, 2616.

(16) Lindblom, G.; Johansson, L.; Arvidson, G. *Biochemistry* **1981**, *20*, 2204.

(17) Cornell, B. A.; Keniry, M. *Biochim. Biophys. Acta* **1983**, *732*, 705.

(18) Hyslop, P. A.; Morel, B.; Sauerheber, R. D. *Biochemistry* **1990**, *29*, 1025.

(19) Smaby, J. M.; Momsen, M. M.; Brockman, H. L.; Brown, R. E. *Biophys. J.* **1997**, *73*, 1492.

(20) Kusumi, A.; Tsuda, M.; Akino, T.; Osnishi, S.; Terayama, Y. *Biochemistry* **1983**, *22*, 1165.

(21) El-Sayed, M. Y.; Guiton, T. A.; Fayer, M. D. *Biochemistry* **1986**, *25*, 4825.

(22) Venable, R. M.; Zhang, Y.; Hardy, B. J.; Pastor, R. W. *Science* **1993**, *262*, 223.

(23) Marrink, S. J.; Berendsen, H. J. C. *J. Phys. Chem.* **1994**, *98*, 4155.

(24) Chiu, S. W.; Clark, M.; Balaji, V.; Subramaniam, S.; Scott, H. L.; Jakobsson, E. *Biophys. J.* **1995**, *69*, 1230.

(25) Tu, K.; Tobias, D. J.; Klein, M. L. *Biophys. J.* **1995**, *69*, 2558.

(26) Feller, S. E.; Zhang, Y.; Pastor, R. W. *J. Chem. Phys.* **1995**, *103*, 10267.

(27) Perera, L.; Essmann, U.; Berkowitz, M. L. *Langmuir* **1996**, *12*, 2625.

(28) López Cascales, J. J.; García de la Torre, J.; Marrink, S. J.; Berendsen, H. J. C. *J. Chem. Phys.* **1996**, *104*, 2713.

(29) Tieleman, D. P.; Berendsen, H. J. C. *J. Chem. Phys.* **1996**, *105*, 4871.

(30) Pasenkiewicz-Gierula, M.; Takaoka, Y.; Miyagawa, H.; Kitamura, K.; Kusumi, A. *J. Phys. Chem. A* **1997**, *101*, 3677.

(31) Husslein, T.; Newns, D. M.; Pattnaik, P. C.; Zhong, Q.; Moore, P. B.; Klein, M. L. *J. Chem. Phys.* **1998**, *109*, 2826.

(32) Chiu, S. W.; Clark, M.; Jakobsson, E.; Subramaniam, S.; Scott, H. L. *J. Comput. Chem.* **1999**, *20*, 1153.

(33) Jedlovszky, P.; Mezei, M. *J. Chem. Phys.* **1999**, *111*, 10770.

(34) Zubrzycki, I. Z.; Xu, Y.; Madrid, M.; Tang, P. *J. Chem. Phys.* **2000**, *112*, 3437.

(35) Jedlovszky, P.; Mezei, M. *J. Am. Chem. Soc.* **2000**, *122*, 5125.

(36) Jedlovszky, P.; Mezei, M. *J. Phys. Chem. B* **2001**, *105*, 3614.

(37) Venable, R. M.; Pastor, R. W. *J. Chem. Phys.* **2002**, *116*, 2663.

(38) Heller, H.; Schaefer, M.; Schulten, K. *J. Phys. Chem.* **1993**, *97*, 8343.

(39) Hyvönen, M. T.; Rantala, T. T.; Ala-Korpela, M. *Biophys. J.* **1997**, *73*, 2907.

(40) Rabinovich, A. L.; Balabaev, N. K. *Proc. SPIE—Int. Soc. Opt. Eng.* **2001**, *4348*, 215.

(41) Murzyn, K.; Róg, T.; Jezierski, G.; Takaoka, Y.; Pasenkiewicz-Gierula, M. *Biophys. J.* **2001**, *81*, 170.

(42) Saiz, L.; Klein, M. L. *Biophys. J.* **2001**, *81*, 204.

(43) Saiz, L.; Klein, M. L. *J. Chem. Phys.* **2002**, *116*, 3052.

(44) Huang, P.; Bertaccini, E.; Loew, G. H. *J. Biomol. Struct. Dyn.* **1995**, *12*, 725.

(45) Bassolino-Klimas, D.; Alper, H. E.; Stouch, T. R. *J. Am. Chem. Soc.* **1995**, *117*, 4118.

(46) Stouch, T. R.; Bassolino, D. In *Biological Membranes*; Merz, K. M., Roux, B., Eds.; Birkhäuser: Boston, 1996; pp 255–280.

(47) López Cascales, J. J.; Hernández Cifre, J. G.; García de la Torre, J. *J. Phys. Chem. B* **1998**, *102*, 625.

(48) Duong, T. H.; Mehler, E. M.; Weinstein, H. J. *Comput. Phys.* **1999**, *151*, 358.

(49) Bandyopadhyay, S.; Tarek, M.; Klein, M. L. *J. Phys. Chem. B* **1999**, *103*, 10075.

(50) Edholm, O.; Nyberg, A. M. *Biophys. J.* **1992**, *63*, 1081.

(51) Robinson, A. J.; Richards, W. G.; Thomas, P. J.; Hann, M. M. *Biophys. J.* **1995**, *68*, 164.

(52) Gabdouline, R. R.; Vanderkooi, G.; Zheng, C. *J. Phys. Chem.* **1996**, *100*, 15942.

(53) Tu, K.; Klein, M. L.; Tobias, D. J. *Biophys. J.* **1998**, *75*, 2147.

(54) Smolyrev, A. M.; Berkowitz, M. L. *Biophys. J.* **1999**, *77*, 2075.

(55) Smolyrev, A. M.; Berkowitz, M. L. *Biophys. J.* **2000**, *78*, 1672.

(56) Pasenkiewicz-Gierula, M.; Róg, T.; Kitamura, K.; Kusumi, A. *Biophys. J.* **2000**, *78*, 1376.

(57) Chiu, S. W.; Jakobsson, E.; Scott, H. L. *J. Chem. Phys.* **2001**, *114*, 5435.

(58) Mezei, M. In *Computational Methods for Macromolecules: Challenges and Applications*; Schlick, T., Gan, H. H., Eds.; Springer: New York, 2002; pp 177–196.

(59) Schlenkirch, M.; Brickmann, J.; MacKerell, A. D., Jr.; Karplus, M. In *Biological Membranes*; Merz, K. M., Roux, B., Eds.; Birkhäuser: Boston, 1996; pp 31–82.

(60) Jorgensen, W. L.; Chandrashekar, J.; Madura, J. D.; Impey, R.; Klein, M. L. *J. Chem. Phys.* **1983**, *79*, 926.

(61) Alper, H. E.; Bassolino, D.; Stouch, T. R. *J. Chem. Phys.* **1993**, *98*, 9798.

(62) Mezei, M. MMC Program at the following URL: <http://inka.mssm.edu/~mezei/mmc>.

(63) Mezei, M. *J. Comput. Phys.* **1983**, *39*, 128.

(64) Jedlovszky, P.; Mezei, M. *Mol. Phys.* **1999**, *96*, 293.

(65) Mavromoustakos, T.; Yang, D. P.; Charalambous, A.; Herbette, L. G.; Makriyannis, A. *Biochim. Biophys. Acta* **1990**, *1024*, 336.

(66) Mezei, M. *J. Comput. Phys.* **1987**, *68*, 237.

(67) Mezei, M. *Mol. Simul.* **1989**, *3*, 301.

(68) Marrink, S. J.; Sok, R. M.; Berendsen, H. J. C. *J. Chem. Phys.* **1996**, *104*, 9090.

(69) Marrink, S. J.; Berendsen, H. J. C. *J. Phys. Chem.* **1996**, *100*, 16729.

(70) Rice, D.; Oldfield, E. *Biochemistry* **1979**, *18*, 3272.

(71) Domínguez, H. *J. Phys. Chem. B* **2002**, *106*, 5915.